Elastic properties and shape of the Piezo dome underlying its mechanosensory function

Supplementary Information

Christoph A. Haselwandter[1], Yusong R. Guo[2], Ziao Fu[2], and Roderick MacKinnon[2]

[1] *Department of Physics and Astronomy and Department of Quantitative and Computational Biology, University of Southern California, Los Angeles, United States.*

[2] *Laboratory of Molecular Neurobiology and Biophysics, Howard Hughes Medical Institute, The Rockefeller University, New York, United States.*

S1 Supplementary figures

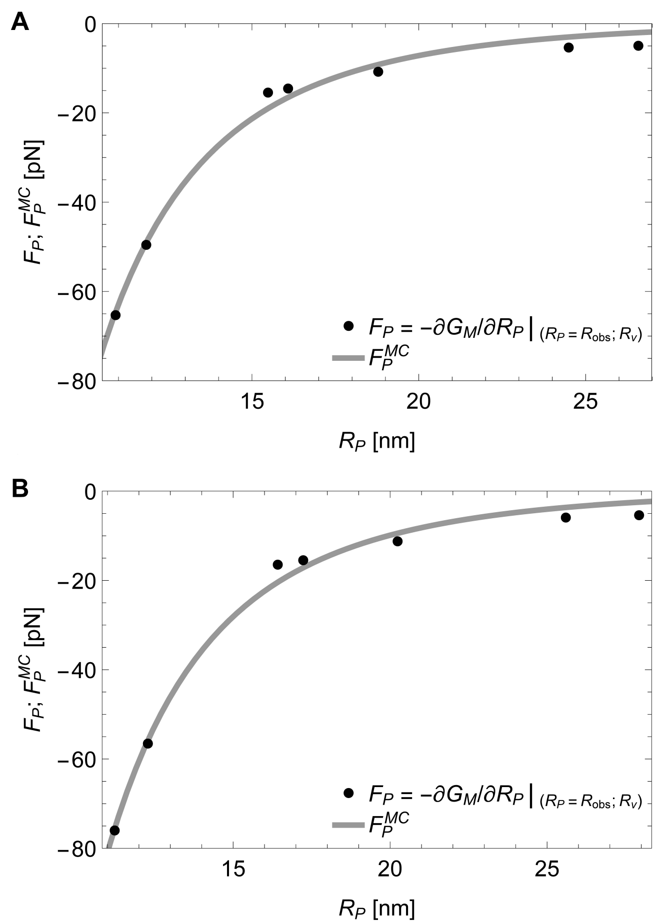

Figure S1: **Mechanics of the Piezo dome.** Same plots as in Fig. 3 of the main text but using, instead of $A_P = 450$ nm^2, the Piezo dome areas (*A*) $A_P = 410$ nm^2 and (*B*) $A_P = 490$ nm^2. We have the fits $K_P = 17 \pm 2.1$ k_BT and $R_P = 40 \pm 11$ nm in panel *A* and $K_P = 18 \pm 2.0$ k_BT and $R_P = 45 \pm 13$ nm in panel *B*.

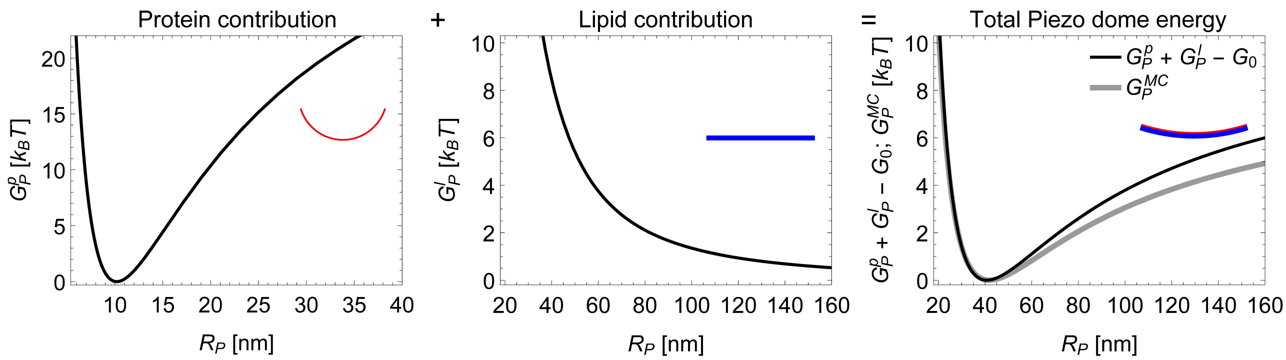

Figure S2: **Toy model of the protein and lipid contributions to Piezo dome mechanics.** The sum of the bending energy of the Piezo protein, $G_P^p(R_P) = 0.25\frac{K_b}{2}A_P\left(\frac{2}{R_P} - \frac{2}{R_0^p}\right)^2$, assuming the protein bending rigidity to be roughly equal to the lipid bilayer bending rigidity K_b and using an intrinsic protein radius of curvature $R_0^p = 10.2$ nm [1] (left panel) and of the bending energy of the lipid bilayer inside the Piezo dome, $G_P^l(R_P) = 0.75\frac{K_b}{2}A_P\left(\frac{2}{R_P}\right)^2$, with bending rigidity K_b and zero intrinsic curvature (middle panel) yields a total Piezo dome energy $G_P^p + G_P^l - G_0$ (black curve in right panel) that is (qualitatively) similar to the mean curvature Piezo dome energy in Eq. (3) of the main text with $K_P \approx 18$ k_BT and $R_0 \approx 42$ nm, $G_P^{MC}(R_P)$ (grey curve in right panel). We set $A_P = 450$ nm^2. In the right panel, we shifted the total Piezo dome energy by the constant G_0 so that $G_P^p + G_P^l - G_0 = 0$ at the value of R_P minimizing $G_P^p + G_P^l$. In the expressions for $G_P^p(R_P)$ and $G_P^l(R_P)$ used here, we assumed that the area of a Piezo dome in a membrane comprises approximately 75% lipid bilayer and 25% protein. The minimum of $G_P^p + G_P^l - G_0$ is thus at $R = 4R_0^p = 40.8$ nm, close to the minimum of $G_P^{MC}(R_P)$ at $R_P = R_0 \approx 42$ nm, with a comparable energy difference to Piezo dome states with $R_P \to \infty$. Differentiating $G_P^p + G_P^l$ with respect to R_P, one finds a force curve for the Piezo dome that is comparable to $F_P^{MC}(R_P)$ in Eq. (4) of the main text (see Fig. 3 of the main text).

S2 Calculating Piezo's membrane footprint

For Figs. 1–3 of the main text, we calculated the shape and elastic energy of the free membrane in Piezo vesicles as described in our companion paper. We calculated the shape and elastic energy of Piezo's membrane footprint in asymptotically planar membranes, Fig. 4 of the main text, based on the theory developed in Ref. [2]. Reference [2] shows that the membrane footprint contribution to Piezo's tension-dependent gating is, in general, comparable to the contribution due to the Piezo dome itself. In this section we summarize the theoretical approach in Ref. [2] used for Fig. 4 of the main text.

As discussed in Ref. [2], the contributions to the shape energy of the Piezo-membrane system in Eq. (5) of the main text arising from Piezo's membrane footprint take the following form in the arclength parameterization of surfaces [3, 4]:

$$G_M = \pi K_b \int_0^{s_b} ds\, r \left[\left(\dot{\psi} + \frac{\sin\psi}{r} \right)^2 + \frac{2}{\lambda^2} \left(1 - \cos\psi\right) \right] , \tag{S1}$$

where s_b is the (fixed) length of the integration domain (membrane compartment size) and $\lambda = \sqrt{K_b/\gamma}$ is the characteristic decay length of membrane shape deformations. Throughout this section, we use the same notation as in our companion paper (see, in particular, Fig. 3*B* of our companion paper). As in Ref. [2], we calculated the extremal membrane footprint shapes, and corresponding elastic footprint energies, implied by Eq. (S1) from the Hamilton equations associated with Eq. (S1), which we solved numerically using a shooting method analogous to the approach used in our companion paper [5, 6]. This shooting method provides an improved version of the numerical approach employed in Ref. [2]—in particular, it allows for a straightforward representation of the boundary conditions fixing the physical properties of Piezo's membrane footprint, and is conveniently and efficiently implemented in *Mathematica* [7].

S2.1 Hamilton equations

Following Ref. [2], the geometric relations $\dot{r} = \cos\psi$ and $\dot{h} = \sin\psi$ can be incorporated into the membrane deformation energy in Eq. (S1) as

$$G_M = \pi K_b \int_0^{s_b} ds L \left(\psi, \dot{\psi}, r, \dot{r}, \dot{h} \right) , \tag{S2}$$

where the Lagrangian is

$$L = r \left[\left(\dot{\psi} + \frac{\sin\psi}{r} \right)^2 + \frac{2}{\lambda^2} \left(1 - \cos\psi\right) \right] + \lambda_r \left(\dot{r} - \cos\psi\right) + \lambda_h \left(\dot{h} - \sin\psi\right) , \tag{S3}$$

in which the Lagrange multipliers $\lambda_r(s)$ and $\lambda_h(s)$ may both vary with s. The generalized momenta p_ψ, p_r, and p_h associated with the generalized displacements ψ, r, and h in Eq. (S2) with Eq. (S3) are defined by [8]

$$p_\psi \equiv \frac{\partial L}{\partial \dot\psi} = 2r\left(\dot\psi + \frac{\sin\psi}{r}\right)\,, \tag{S4}$$

$$p_r \equiv \frac{\partial L}{\partial \dot r} = \lambda_r\,, \tag{S5}$$

$$p_h \equiv \frac{\partial L}{\partial \dot h} = \lambda_h\,. \tag{S6}$$

It is convenient to solve the Hamilton equations for Eq. (S2) with Eq. (S3) in dimensionless form. Denoting the characteristic spatial scale by L_c, we thus define the following dimensionless variables:

$$\bar s \equiv \frac{1}{L_c}s\,, \quad \bar\psi \equiv \psi\,, \quad \bar r \equiv \frac{1}{L_c}r\,, \quad \bar h \equiv \frac{1}{L_c}h\,, \tag{S7}$$

$$\bar p_\psi \equiv p_\psi\,, \quad \bar p_r \equiv L_c\, p_r\,, \quad \bar p_h \equiv L_c p_h\,, \quad \bar\lambda = \frac{1}{L_c}\lambda\,. \tag{S8}$$

In terms of the dimensionless variables in Eqs. (S7) and (S8), the Hamilton equations associated with Piezo's membrane footprint [2] are given by

$$\bar\psi' = \frac{\bar p_\psi}{2\bar r} - \frac{\sin\bar\psi}{\bar r}\,, \tag{S9}$$

$$\bar r' = \cos\bar\psi\,, \tag{S10}$$

$$\bar h' = \sin\bar\psi\,, \tag{S11}$$

$$\bar p_\psi' = \left(\frac{\bar p_\psi}{\bar r} - \bar p_h\right)\cos\bar\psi + \left(\frac{2\bar r}{\bar\lambda^2} + \bar p_r\right)\sin\bar\psi\,, \tag{S12}$$

$$\bar p_r' = \frac{\bar p_\psi}{\bar r}\left(\frac{\bar p_\psi}{4\bar r} - \frac{\sin\bar\psi}{\bar r}\right) + \frac{2}{\bar\lambda^2}\left(1-\cos\bar\psi\right)\,, \tag{S13}$$

$$\bar p_h' = 0\,, \tag{S14}$$

where we denote with f' the derivative of some function f with respect to $\bar s$, $f' \equiv df/d\bar s$.

S2.2 Boundary conditions

In order to find the dominant (lowest-energy) shape and associated energy of Piezo's membrane footprint we need to solve Eqs. (S9)–(S14) subject to suitable boundary conditions. As discussed in our companion paper, the general form of these boundary conditions can be derived from the calculus of variations [9–11]. Following Ref. [2], the boundary conditions for Piezo's membrane footprint in asymptotically planar membranes are, in dimensionless form, given by

$$\bar\psi(0) = \alpha\,, \tag{S15}$$

$$\bar\psi(\bar s_b) = 0\,, \tag{S16}$$

$$\bar r(0) = \bar R_P \sin\alpha\,, \tag{S17}$$

$$\bar{h}(0) = -\bar{R}_P \cos\alpha\,, \tag{S18}$$

$$\bar{p}_r(\bar{s}_b) = 0\,, \tag{S19}$$

$$\bar{p}_h(0) = 0\,, \tag{S20}$$

where $\bar{s}_b = s_b/L_c$, $\bar{R}_P = R_P/L_c$, and the Piezo dome (cap) contact angle

$$\alpha = \cos^{-1}\left(1 - \frac{A_P}{2\pi R_P^2}\right)\,. \tag{S21}$$

We used here the Piezo dome (cap) area $A_P = 450$ nm^2. The boundary condition in Eq. (S20) is obtained from Eq. (S14) together with the natural (zero-force) boundary condition $\bar{p}_h(\bar{s}_b) = 0$ [2]. Based on Eq. (S17) we use here $L_c = R_P \sin\alpha$ as the characteristic spatial scale of the system, resulting in $\bar{r}(0) = 1$ and $\bar{h}(0) = -\cot\alpha$ in Eqs. (S17) and (S18), respectively. We set $\bar{s}_b = 5\bar{\lambda}$ to calculate Piezo's membrane footprint in large (asymptotically planar) membranes.

S2.3 Solving the Hamilton equations

The six Hamilton equations in Eqs. (S9)–(S14) must be solved subject to the six boundary conditions in Eqs. (S15)–(S20), which we achieve through a shooting method analogous to that employed in our companion paper. In particular, we directly impose the initial conditions in Eqs. (S15), (S17), (S18), and (S20), and impose the boundary conditions at $\bar{s} = \bar{s}_b$ in Eqs. (S16) and (S19) by introducing the variables $\bar{p}_{\psi;0}$ and $\bar{p}_{r;0}$,

$$\bar{p}_\psi(0) = \bar{p}_{\psi;0}\,, \tag{S22}$$

$$\bar{p}_r(0) = \bar{p}_{r;0}\,. \tag{S23}$$

We determine the values of $\bar{p}_{\psi;0}$ and $\bar{p}_{r;0}$ in Eqs. (S22) and (S23) from the boundary conditions in Eqs. (S16) and (S19) through a shooting method. In this shooting method, the values of $\bar{p}_{\psi;0}$ and $\bar{p}_{r;0}$ are iteratively adjusted so that Eqs. (S16) and (S19) are satisfied. Similarly as described in our companion paper, this is achieved conveniently and efficiently in *Mathematica* [7] by nesting the *NDSolve*-command, used to numerically solve Eqs. (S9)–(S14) subject to Eqs. (S15), (S17), (S18), (S20), (S22), and (S23), inside the *FindRoot*-command, used to adjust the values of $\bar{p}_{\psi;0}$ and $\bar{p}_{r;0}$ in Eqs. (S22) and (S23) so as to satisfy Eqs. (S16) and (S19). To initialize the numerical optimization carried out by the *FindRoot*-command, it is thereby necessary to specify starting values for $\bar{p}_{\psi;0}$ and $\bar{p}_{r;0}$. For instance, for the parameter values $R_P \approx 42$ nm and $\gamma = 0.01$ k_BT/nm^2 used in the left panel of Fig. 4*A* of the main text, suitable starting values of $\bar{p}_{\psi;0}$ and $\bar{p}_{r;0}$ are $(\bar{p}_{\psi;0}, \bar{p}_{r;0}) \approx (-0.063, -0.014)$. When carrying out a series of related shooting calculations with only minor changes to the constraints imposed on Piezo's membrane footprint—for instance, to evaluate G_M as a function of γ—it is generally convenient to initialize $\bar{p}_{\psi;0}$ and $\bar{p}_{r;0}$ using the optimized values of $\bar{p}_{\psi;0}$ and $\bar{p}_{r;0}$ obtained for a 'nearby' (the preceding) solution. As also noted in our companion paper, a general caveat is that the shooting method does not necessarily yield a unique solution to boundary value problems such as studied here. After solving Eqs. (S9)–(S14) subject to Eqs. (S15)–(S20), we substitute these solutions into Eq. (S1) and evaluate the integral, to calculate the (stationary) elastic energy of Piezo's membrane footprint.

References

[1] Y. R. Guo and R. MacKinnon. Structure-based membrane dome mechanism for Piezo mechanosensitivity. *eLife*, 6:e33660, 2017.

[2] C. A. Haselwandter and R. MacKinnon. Piezo's membrane footprint and its contribution to mechanosensitivity. *eLife*, 7:e41968, 2018.

[3] W. Kühnel. *Differential Geometry*, volume 77. American Mathematical Society, 3rd edition, 2015.

[4] M. P. do Carmo. *Differential Geometry of Curves and Surfaces.* Dover Publications, New York, 2016.

[5] R. L. Burden and J. D. Faires. *Numerical Analysis.* Brooks/Cole, Cengage Learning, Boston, 9th edition, 2011.

[6] W. Gautschi. *Numerical Analysis.* Springer Science & Business Media, New York, 2nd edition, 2012.

[7] *Mathematica 11.2.* Wolfram Research, Inc., Champaign, IL, 2017.

[8] T. W. B. Kibble and F. H. Berkshire. *Classical Mechanics.* Imperial College Press, London, 5th edition, 2004.

[9] R. Courant and D. Hilbert. *Methods of Mathematical Physics*, volume 1. Interscience Publishers, Inc., New York, 1st edition, 1953.

[10] J. Mathews and R. L. Walker. *Mathematical Methods of Physics.* W. A. Benjamin, New York, 1st edition, 1964.

[11] B. van Brunt. *The Calculus of Variations.* Springer, New York, 2004.